

# Fringe-locking method for the weak equivalence principle test by simultaneous dual-species atom interferometers

Xiao-Chun Duan,<sup>1</sup> Xiao-Bing Deng,<sup>1</sup> De-Kai Mao,<sup>1</sup>  
Min-Kang Zhou,<sup>1</sup> Cheng-Gang Shao,<sup>1</sup> and Zhong-Kun Hu<sup>1,\*</sup>

<sup>1</sup>MOE Key Laboratory of Fundamental Physical Quantities Measurements, School of Physics,  
Huazhong University of Science and Technology, Wuhan 430074, People's Republic of China

compiled: March 7, 2016

We theoretically investigate the application of the fringe-locking method (FLM) in the dual-species quantum test of the weak equivalence principle (WEP). With the FLM, the measurement is performed invariably at the midfringe, and the extraction of the phase shift for atom interferometers is linearized. For the simultaneous interferometers, this linearization enables a good common-mode rejection of vibration noise, which is usually the main limit for high precision WEP tests of dual-species kind. We note that this method also allows for an unbiased determination of the gravity accelerations difference, which meanwhile is readily to be implemented.

## 1. Introduction

Benefit from the highly developed atom interferometry technology, cold atoms, possessing both internal and external degrees of freedom, become ideal probes in many precision measurements. They have been successfully used in measuring gravity acceleration [1–10], gravity gradient [7, 8, 11–16], rotation [17–23], magnetic field gradient [24–27], etc. Atom interferometers also play an important role in fundamental physics, such as the measurement of fine structure constant, the determination of gravitational constant  $G$  [28–30], and the test of the weak equivalence principle (WEP) [2, 31–36].

WEP, as one of the cornerstones of Einstein's general relativity, states that all masses fall in the same way in a gravitational field regardless of their internal structure and composition. Verifications of WEP using macroscopic masses have achieved a level of  $10^{-13}$  [37, 38], while the best level for testing WEP on quantum basis is at the level of  $10^{-9}$  [2]. Testing WEP using microscopic particles still stimulated wide interest since the neutron interferometer [39]. The reason is that, quantum objects offer more possibilities to break WEP and meanwhile they also afford potentially higher precision and well defined properties [34, 40, 41]. Up to date, WEP tests on quantum basis have been performed using atoms versus macroscopic bodies [2] or other atom species [34], using single-specie atoms in different hyperfine levels [31] or in different spin orientations [42], and using bosonic atoms versus fermionic atoms [35], achieving a level of  $10^{-7}$ . In these tests, the corresponding gravity accelerations are usually independently measured and then compared, in which situation the vibration noise

cannot be common-mode rejected. Under this circumstance, WEP test using simultaneous dual-species atom interferometers is particularly interesting for its intrinsic capability of common-mode suppressing the vibration noise [32, 36]. WEP tests of this kind have already been performed by several groups, achieving a level of  $10^{-8}$  [36], and tests with higher precision are under development [43, 44] or have been proposed [45, 46].

However, common-mode rejection of vibration noise in WEP tests of dual-species kind, especially using non-isotope species, is not so direct as that, for example, in atom gradiometers. In the operation of coupled interferometers using the same atoms, it is mature to extract the differential phase shift  $\Delta\Phi$  in a common-mode noises immune way by the ellipse fit method [47] or Bayesian estimation [48–50]. But in WEP tests of dual-species kind, the scale factors  $S_j \cong k_j^{\text{eff}} T_j^2$  are usually different for the two interferometers, which originates from the different effective Raman wave vectors used for the atom species  $j = 1$  and  $2$  when the pulses separation times  $T_j$  are the same. The different scale factors cause two aspects of complexity in the signal extraction of WEP tests. Firstly, the interested signal  $\Delta g \equiv g_1 - g_2$  is not proportional to the differential phase shift, which excludes the direct extraction of  $\Delta g$  using usual ellipse fit method or Bayesian estimation. Secondly, the induced phase fluctuations by vibration noise are not the same for the two interferometers, which increases the difficulty to common-mode suppress the vibration noise. The scale factors can be made the same by using different values for the pulses separation times  $T_j$ , which is particularly favorable in the case of the ratio  $r \equiv k_2^{\text{eff}}/k_1^{\text{eff}}$  close to unity [49]. However, in this situation, the experienced vibration noise is not exactly the same for the two interferometers, which thus excludes the possibility of perfect common-mode suppression. It is also proposed to

---

\* zkhu@hust.edu.cn

simultaneously measure the vibration noise by an auxiliary sensor and then reconstruct the fringes [51, 52]. The effectiveness of this method depends on the quality of the correlation between real and measured vibrations, which is hard to ensure when the aimed precision of the WEP test is beyond the intrinsic noise of state-of-art vibrations sensors. This problem may also be mathematically resolved by improved ellipse fit method, Bayesian estimation or direct phase extraction [33, 50, 52]. However, these solutions either require complex computation (sometimes even causing a bias result) or suffer from the trouble of separating the WEP violation signal from total differential phase shift.

It is already clear that the gravity acceleration or the vibration induced phase shift is linear to  $k_j^{\text{eff}}$ , and we further note it is the conventional non-linear phase extraction process from the interference fringe that complicates the WEP violation signal separation and the vibration noise common-mode rejection. Actually, the fringe-locking method (FLM) has already been adopted formerly for single atom interferometers [53–56] and recently for coupled interferometers [16], by which the signal extraction of the interferometer can be linearized as already exploited in single atom interferometer. In this work, we propose to operate the dual-species atom interferometers in the fringe-locking mode to linearize the signal extraction, which promises a good common-mode rejection of vibration noise, especially in the case of low level vibration noise. We note that, in the WEP test of dual-species kind, it only needs a change in the control of the Raman lasers effective frequencies to perform the fringe-locking method, and the corresponding signal extraction is quite direct. Moreover, this fringe-locking method allows for an unbiased determination of  $\Delta g$ .

## 2. Review of Fringe-Locking Method

In light pulses atom interferometers, the interference pattern is usually manifested as the variation of the transition probability between the two ground levels of the atom. And the transition probability  $P$  is typically expressed as [1, 3]

$$P = A + B \cos(\varphi + \varphi_m), \quad (1)$$

which forms a cosine fringe when the controllable  $\varphi$  is scanned. In Eq. (1),  $A$  is the fringe offset,  $B$  is the fringe amplitude, and  $\varphi_m$  indicates the phase shift induced by the physical quantity to be measured. In conventional method, a full cosine fringe is obtained by scanning  $\varphi$  step by step, as shown in Fig. 1(a), and  $\varphi_m$  is then acquired by a cosine fitting. Alternatively, the FLM can be adopted [53–55], as shown in Fig. 1(b). In the fringe-locking approach, the appropriate value of  $\varphi$ , denoted as  $\varphi^0$ , is found to make  $\varphi + \varphi_m \sim 2n\pi$  (where  $n$  is an integer). Then  $\varphi$  is modulated by  $\pm\pi/2$  with respect to the center of  $\varphi^0$  so that the measurement is always performed at midfringe, alternately to the right and to the left side of the central fringe. In this case, the transition probabilities  $P$  for every two consecutive launches can

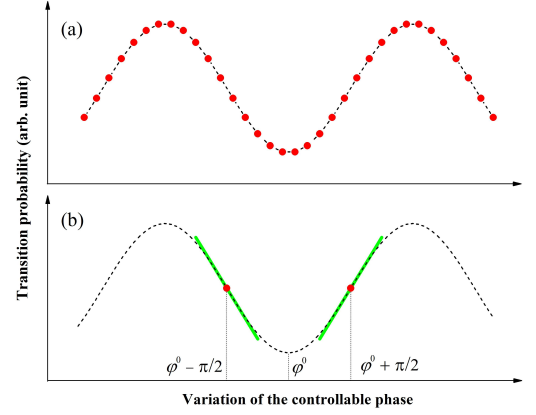


Fig. 1. (color online) Different methods to operate the interferometer, with (a) for recording full fringes and (b) for performing measurements at midfringe. In the conventional method, the phase is scanned step by step, while in the FLM, the phase is modulated by  $\pm\pi/2$  with respect to an appropriate center, denoted as  $\varphi^0$  here. The dash lines are here to guide the eyes. And the two thick green lines are the tangent lines of the midfringe, which show good approximation for the fringe near the center.

be expressed as

$$P[2l-1] = A + B \cos(\varphi^0 + \varphi_m - \pi/2), \quad (2a)$$

$$P[2l] = A + B \cos(\varphi^0 + \varphi_m + \pi/2), \quad (2b)$$

where  $l$  ( $l = 1, 2, 3, \dots$ ) denotes the index of modulating cycles. The difference between  $P[2l-1]$  and  $P[2l]$  could be used as a criterion of whether  $\varphi^0 + \varphi_m = 2n\pi$  is fulfilled, which thus enables feedback control of  $\varphi^0$ . According to the linear approximating of Eq. (2) at midfringe, the correction can be expressed as

$$\delta(\varphi^0) = (P[2l] - P[2l-1])/2B, \quad (3)$$

where the fringe amplitude  $B$  must be known in advance by scanning full fringe. Once the corrections are made to form a closed feedback loop, the equation  $\varphi^0 + \varphi_m = 2n\pi$  is supposed to be enable, from which the value of the interested  $\varphi_m$  can be deduced from  $\varphi^0$  in a linear way. It is shown in Eq. (3) that when the interferometers is operated at the midfringe, the measurement works in a linear region. This linearization character is helpful for signal extraction in the WEP test of dual-species kind, as will be discussed detailedly in the following section.

## 3. Application in WEP Test

In the above section, the fringe-locking approach for single interferometer is illuminated, and the Raman laser phase is convenient to control, which thus usually plays the role of  $\varphi$ . Generally speaking, one needs two independent controllable phases to simultaneously lock two interferometers. In Ref. 16, in addition to Raman laser

phase, the phase shift due to magnetic field gradient is explored as the other controllable phase for an atom gravity gradiometer. In WEP test using simultaneous dual-species atom interferometers, there are already two independent groups of Raman lasers (usually one group used for one specie atom), and thus it is natural to explore the two controllable Raman laser phases for fringe locking.

For each specie atom interferometer using  $\pi/2 - \pi - \pi/2$  Raman pulses scheme, the controllable phase  $\varphi$ , namely the Raman lasers phase, can be expressed as [33, 50, 52, 57]

$$\varphi_j = \alpha_j(T_j + 2\tau_j)(T_j + 4\tau_j/\pi) \equiv \alpha_j f_{\text{DC}}(T_j, \tau_j), \quad (4)$$

where  $\alpha_j$  is the chirp rate of the effective Raman laser frequency used to compensate the Doppler shift due to gravity, and  $\tau_j$  is the  $\pi/2$  pulse duration. With the Raman pulses duration effect neglected,  $f_{\text{DC}}(T_j, \tau_j)$  just simplifies to  $T_j^2$ . And the interested phase  $\varphi_m$ , namely the phase related to the gravity acceleration, can be expressed as [33, 50, 52, 57]

$$(\varphi_m)_j = k_j^{\text{eff}} g_j f_{\text{DC}}(T_j, \tau_j), \quad (5)$$

where the gravity acceleration of  $j$  specie atoms is denoted as  $g_j$  to account for possible WEP violation. In order to clearly manifest the ability of common-mode rejection with FLM, the phase due to vibration is explicitly included in the total phase shift, which can be expressed as [33, 50, 52, 57]

$$\begin{aligned} (\varphi_{\text{vib}})_j &= k_j^{\text{eff}} \int_{-\infty}^{\infty} \xi(t - (t_i)_j) \int_{-\infty}^t a(t') dt' dt \\ &\equiv k_j^{\text{eff}} h(T_j, \tau_j; a(t), (t_i)_j), \end{aligned} \quad (6)$$

where  $\xi(t)$  is the sensitivity function [58], and  $t_i$  is the central time of the interfering progress for the  $i$ -th shot measurement. We note that both  $f_{\text{DC}}(T_j, \tau_j)$  and  $h(T_j, \tau_j; a(t), t_i)$  are irrelative to  $k_j^{\text{eff}}$  [33, 50, 52, 57]. And in the case of identical pulses separation time (namely  $T_1 = T_2 \equiv T$ ), identical effective Rabi frequencies (thus  $\tau_1 = \tau_2 \equiv \tau$ ), and simultaneous interferometers (thus  $(t_i)_1 = (t_i)_2 \equiv t_i$  as well as experiencing the same vibration noise  $a(t)$ ), they are identical for the dual-species atom interferometers. This is exactly the situation we hope (and also are able to) manage to achieve, and here we then abbreviate  $f_{\text{DC}}(T, \tau)$  and  $h(T, \tau; a(t), t_i)$  as  $f_{\text{DC}}$  and  $h[l]$ , respectively.

Once the appropriate value of Raman laser phase, denoted as  $\varphi_j^0$ , are found to make  $\varphi_j + (\varphi_m)_j \sim 2n_j\pi$  for each interferometers, the Raman laser phases are then modulated by  $\pm\pi/2$ . The corresponding transition probabilities for the two interferometers for every two consecutive launches can be expressed as

$$\begin{aligned} P_j[2l-1] &= A_j + B_j \cos(\varphi_j^0 + k_j^{\text{eff}} g_j f_{\text{DC}} \\ &\quad + k_j^{\text{eff}} h[2l-1] - \pi/2), \end{aligned} \quad (7a)$$

$$\begin{aligned} P_j[2l] &= A_j + B_j \cos(\varphi_j^0 + k_j^{\text{eff}} g_j f_{\text{DC}} \\ &\quad + k_j^{\text{eff}} h[2l] + \pi/2). \end{aligned} \quad (7b)$$

And as same as in single interferometer, the correction is made as

$$\delta((\varphi_j^0)[l]) = (P_j[2l] - P_j[2l-1])/2B_j, \quad (8)$$

where  $l$  denotes the  $l$ -th correction (the index of  $\varphi_j^0$  is explicitly indicated here). The  $(l+1)$ -th phase modulation center will be  $(\varphi_j^0)[l+1] = (\varphi_j^0)[l] + \delta((\varphi_j^0)[l])$ . And for single interferometer, the  $l$ -th measured value of the gravity acceleration is then expressed as  $(g_{\text{meas}})_j[l] = (2n_j\pi - \varphi_j^0[l] - \delta((\varphi_j^0)[l]))/k_j^{\text{eff}} f_{\text{DC}}$ . This measured value is obviously affected by the vibration noise, which can be actually explicitly deduced from the linear approximation of Eq. (7) at midfringe, namely

$$(g_{\text{meas}})_j[l] = g_j + (h[2l-1] + h[2l])/2f_{\text{DC}}. \quad (9)$$

However, the measured WEP violation signal is the difference of the measured gravity accelerations, which is then expressed as

$$(\Delta g)_{\text{meas}}[l] \equiv (g_{\text{meas}})_1[l] - (g_{\text{meas}})_2[l] = g_1 - g_2, \quad (10)$$

which is exactly the possible WEP violation signal one searches for. It is clearly shown from Eq. (10) that the FLM promises a perfect common-mode rejection of vibration noise within the first order approximation for WEP tests using simultaneous dual-species atom interferometers. And this common-mode rejection capability profits from the linearized signal extraction.

#### 4. Simulation and Result

Eq. (9) is based on the linear approximation of the measurement equation Eq. (7), and so is the consequent common-mode rejection. Actually, vibration noise would cause a departure of the measurement point from midfringe, which would then affect the linear approximation. It is easily imaged that this affection will increase with the noise level. And since the vibration noise induced phases for the two interferometers are different, the relative sites of the measurement points at respective fringe are also different, which will limit the common-mode rejection capability of this fringe-locking method. The rejection capability will be investigated here by numerical simulation. For simplicity, in the simulation the transition probabilities are re-written as

$$P_1 = A_1 + B_1 \cos(\varphi_1 + (\varphi_g)_1 + \varphi_{\text{vib}}), \quad (11a)$$

$$P_2 = A_2 + B_2 \cos(\varphi_2 + r(\varphi_g)_2 + r\varphi_{\text{vib}}), \quad (11b)$$

where  $(\varphi_g)_1$  is equivalent to  $(\varphi_m)_1$ , and  $(\varphi_g)_2$  is defined as  $(\varphi_g)_2 \equiv k_1^{\text{eff}} g_2 f_{\text{DC}}$ . With this redefinition,  $(\varphi_g)_1 = (\varphi_g)_2$  in the absence of WEP violation. The vibration noise is simulated by randomly drawing the

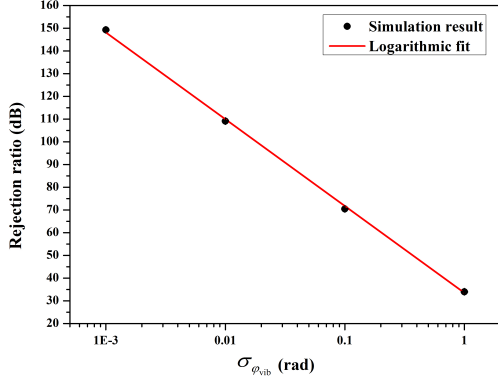


Fig. 2. (color online) Variation of the rejection ratio along the vibration noise level. In this group of simulation, the gravity induced phase is set as  $(\varphi_g)_1 = (\varphi_g)_2 = 2$  rad, and the ratio for the effective Raman wave vector is set as 780/767, the value for the dual-species of  $^{39}\text{K}$  versus  $^{87}\text{Rb}$ .

values of  $\varphi_{\text{vib}}$  in a Gaussian distribution with a standard deviation of  $\sigma_{\varphi_{\text{vib}}}$ . To simulate the fringe locking, the Raman laser phase  $\varphi_1$  ( $\varphi_2$ ) is modulated by  $\pm\pi/2$  with a center of  $\varphi_1^0$  ( $\varphi_2^0$ ), and the corrections for every two consecutive launches is made as Eq. (8) (The initial values of  $\varphi_1$  and  $\varphi_2$  are  $-(\varphi_g)_1$  and  $-(\varphi_g)_2$ , respectively). The corresponding measured phase shifts due to gravity acceleration are then  $(\varphi_g)_1^{\text{meas}} = -\varphi_1^0$  and  $(\varphi_g)_2^{\text{meas}} = -\varphi_2^0/r$ , from which the interested possible WEP violation signal can be deduced as  $\Delta\Phi_g \equiv (\varphi_g)_1 - (\varphi_g)_2 = -(\varphi_1^0 - \varphi_2^0/r)$ .

In the numerical simulation, the dependence of the common-mode rejection efficiency on the vibration noise level (characterized by  $\sigma_{\varphi_{\text{vib}}}$ ) and the ratio of the effective Raman wave vector (characterized by  $r$ ) is investigated. For each  $\sigma_{\varphi_{\text{vib}}}$  and  $r$ ,  $10^4$  modulation cycles are simulated for the two interferometers, in which process  $2 \times 10^4$  pairs ( $P_1, P_2$ ) are generated with  $A_1 = A_2 = 0.5$  and  $B_1 = B_2 = 0.5$  and  $10^4$  pairs  $((\varphi_g)_1^{\text{meas}}, (\varphi_g)_2^{\text{meas}})$  are obtained. The influence of the vibration noise on the interested signal is characterized by the Allan deviation of the  $\Delta\Phi_g$ , which is calculated by the obtained pairs  $((\varphi_g)_1^{\text{meas}}, (\varphi_g)_2^{\text{meas}})$ . Since the simulated vibration noise is white noise, the calculated Allan deviation of  $\Delta\Phi_g$ , denoted as  $\sigma_{\Delta\Phi_g}(N)$ , scales down by the inverse square-root of the number of measurement, namely  $\sigma_{\Delta\Phi_g}(N) = \sigma_{\Delta\Phi_g}^1/\sqrt{N}$ . Here  $N$  denotes the number of measurements, and  $\sigma_{\Delta\Phi_g}^1$  stands for the measurement sensitivity, which is obtained by white noise model fitting of  $\sigma_{\Delta\Phi_g}(N)$  versus  $N$ .

The efficiency of the common-mode noise rejection is characterized by the rejection ratio  $\sigma_{\varphi_{\text{vib}}}/\sigma_{\Delta\Phi_g}^1$ . The simulation result for the dependence of the rejection ratio on the vibration noise level  $\sigma_{\varphi_{\text{vib}}}$  is shown in Fig. 2. According to the logarithmic fit in Fig. 2, the rejection ratio scales by  $-38.2(1)$  dB per octave, which is very close to the expected value of  $-40$  dB per octave as a

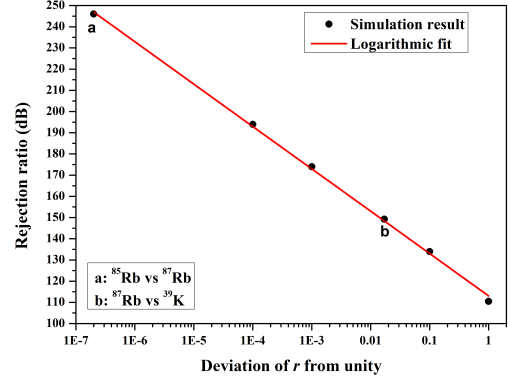


Fig. 3. (color online) Dependence of the rejection ratio on the ratio of the effective Raman wave vector. The ratios for dual-species of  $^{87}\text{Rb}$  versus  $^{85}\text{Rb}$  and  $^{39}\text{K}$  versus  $^{87}\text{Rb}$  are explicitly displayed. In this group of simulation, the gravity induced phase is set as  $(\varphi_g)_1 = (\varphi_g)_2 = 2$  rad, and the vibration noise level is fixed at  $\sigma_{\varphi_{\text{vib}}} = 1$  mrad.

result of the third order expansion of the sinusoid function. This means that the common-mode noise rejection capability of the fringe-locking method improves quite fast as the vibration noise decreases. This simulation also tells that even if the vibration noise is as large as 1 rad, there is still about 33 dB rejection ratio for the  $^{39}\text{K}$  versus  $^{87}\text{Rb}$  dual-species interferometers.

The simulation for different  $r$  is then performed with a fixed vibration noise level of  $\sigma_{\varphi_{\text{vib}}} = 1$  mrad. The result is shown in Fig. 3, which also shows a logarithmic relation. According to the logarithmic fit, the rejection ratio scales down by  $-19.98(4)$  dB per octave. It is shown that even if the deviation of the ratio from unity is as large as 1, there is still about 110 dB rejection ratio for  $\sigma_{\varphi_{\text{vib}}} = 1$  mrad.

In addition to common-mode noise rejection capability, the bias of the extracted  $\Delta\Phi_g$  is also much concerned. We have checked that the average value of  $\Delta\Phi_g$  extracted by this fringe-locking method is exactly equal to the differential value of the set  $(\varphi_g)_1$  and  $(\varphi_g)_2$ , whatever the vibration noise level (as long as  $\sigma_{\varphi_{\text{vib}}} \leq 1$  rad) and the ratio of the effective Raman wave vector are.

## 5. Discussion and Conclusion

The simulation for different fringe amplitudes of the two interferometers (namely  $B_1 \neq B_2$ ) is also performed, and the dependence of the rejection ratio on  $\sigma_{\varphi_{\text{vib}}}$  and  $r$  doesn't change. This is consistent with our knowledge. In the presence of only phase noises, the absolute value of the amplitude doesn't matter much for the FLM as long as it is exactly known. In actual experiment, the fringe amplitudes of the two interferometers are pre-determined by scanning the full fringe and then performing cosine fittings. In the fringe-locking mode, the realtime information about the fringe amplitudes is lost, of which possible drift will affect the fringe-locking. This can be resolved by occasionally switching back to



the full-fringe recording mode to get renewed fringe amplitudes.

In conclusion, we have shown the capability of common-mode noise rejection using fringe-locking method in WEP test by simultaneous dual-species atom interferometers. We note that it is quite convenient to perform this method in the dual-species interferometers, and it is also quite direct to extract the signal. Of importance, this signal extraction approach allows for an unbiased determination of the gravity accelerations difference, and affords a good common-mode noise rejection, especially in the low vibration noise level. This will thus greatly alleviate the demand for the vibration noise isolation in WEP test of dual-species kind.

### Acknowledgements

This work is supported by the National Natural Science Foundation of China (Grants No. 41127002, No. 11574099, and No. 11474115) and the National Basic Research Program of China (Grant No. 2010CB832806).

### References

- [1] M. Kasevich and S. Chu, Atomic interferometry using stimulated raman transitions, *Phys. Rev. Lett.* **67**, 181 (1991).
- [2] A. Peters, K. Y. Chung, and S. Chu, Measurement of gravitational acceleration by dropping atoms, *Nature* **400**, 849-852 (1999).
- [3] A. Peters, K. Y. Chung, and S. Chu, High-precision gravity measurements using atom interferometry, *Metrologia* **38**, 25 (2001).
- [4] J. Le Gouët, T. Mehlstäubler, J. Kim, S. Merlet, A. Clairon, A. Landragin, and F. P. Dos Santos, Limits to the sensitivity of a low noise compact atomic gravimeter, *Appl. Phys. B* **92**, 133-144 (2008).
- [5] H. Müller, S.-w. Chiow, S. Herrmann, S. Chu, and K.-Y. Chung, Atominterferometry tests of the isotropy of post-newtonian gravity, *Phys. Rev. Lett.* **100**, 031101 (2008).
- [6] M.-K. Zhou, Z.-K. Hu, X.-C. Duan, B.-L. Sun, L.-L. Chen, Q.-Z. Zhang, and J. Luo, Performance of a cold-atom gravimeter with an active vibration isolator, *Phys. Rev. A* **86**, 043630 (2012).
- [7] Y. Bidel, O. Carraz, R. Charrière, M. Cadoret, N. Zahzam, and A. Bresson, Compact cold atom gravimeter for field applications, *Appl. Phys. Lett.* **102**, 144107 (2013).
- [8] P. Altin, M. Johnsson, V. Negnevitsky, G. Dennis, R. Anderson, J. Debs, S. Szigeti, K. Hardman, S. Bennetts, G. McDonald et al., Precision atomic gravimeter based on bragg diffraction, *New J. Phys.* **15**, 023009 (2013).
- [9] Z.-K. Hu, B.-L. Sun, X.-C. Duan, M.-K. Zhou, L.-L. Chen, S. Zhan, Q.-Z. Zhang, and J. Luo, Demonstration of an ultrahigh-sensitivity atominterferometry absolute gravimeter, *Phys. Rev. A* **88**, 043610 (2013).
- [10] P. Gillot, O. Francis, A. Landragin, F. P. Dos Santos, and S. Merlet, Stability comparison of two absolute gravimeters: optical versus atomic interferometers, *Metrologia* **51**, L15 (2014).
- [11] M. Snadden, J. McGuirk, P. Bouyer, K. Haritos, and M. Kasevich, Measurement of the earths gravity gradient with an atom interferometerbased gravity gradiometer, *Phys. Rev. Lett.* **81**, 971 (1998).
- [12] J. McGuirk, G. Foster, J. Fixler, M. Snadden, and M. Kasevich, Sensitive absolute-gravity gradiometry using atom interferometry, *Phys. Rev. A* **65**, 033608 (2002).
- [13] F. Sorrentino, Q. Bodart, L. Cacciapuoti, Y.-H. Lien, M. Prevedelli, G. Rosi, L. Salvi, and G. Tino, Sensitivity limits of a raman atom interferometer as a gravity gradiometer, *Phys. Rev. A* **89**, 023607 (2014).
- [14] N. Yu, J. Kohel, J. Kellogg, and L. Maleki, Development of an atominterferometer gravity gradiometer for gravity measurement from space, *Appl. Phys. B* **84**, 647-652 (2006).
- [15] F. Sorrentino, A. Bertoldi, Q. Bodart, L. Cacciapuoti, M. De Angelis, Y.-H. Lien, M. Prevedelli, G. Rosi, and G. Tino, Simultaneous measurement of gravity acceleration and gravity gradient with an atom interferometer, *Appl. Phys. Lett.* **101**, 114106 (2012).
- [16] X.-C. Duan, M.-K. Zhou, D.-K. Mao, H.-B. Yao, X.-B. Deng, J. Luo, and Z.-K. Hu, Operating an atom-interferometry-based gravity gradiometer by the dual-fringe-locking method, *Phys. Rev. A* **90**, 023617 (2014).
- [17] A. Lenef, T. D. Hammond, E. T. Smith, M. S. Chapman, R. A. Rubenstein, and D. E. Pritchard, Rotation sensing with an atom interferometer, *Phys. Rev. Lett.* **78**, 760 (1997).
- [18] T. Gustavson, P. Bouyer, and M. Kasevich, Precision rotation measurements with an atom interferometer gyroscope, *Phys. Rev. Lett.* **78**, 2046 (1997).
- [19] S. Wu, E. Su, and M. Prentiss, Demonstration of an area-enclosing guided-atom interferometer for rotation sensing, *Phys. Rev. Lett.* **99**, 173201 (2007).
- [20] A. Gauguier, B. Canuel, T. Lèveque, W. Chaibi, and A. Landragin, Characterization and limits of a cold-atom sagnac interferometer, *Phys. Rev. A* **80**, 063604 (2009).
- [21] J. Stockton, K. Takase, and M. Kasevich, Absolute geodetic rotation measurement using atom interferometry, *Phys. Rev. Lett.* **107**, 133001 (2011).
- [22] G. Tackmann, P. Berg, C. Schubert, S. Abend, M. Gilowski, W. Ertmer, and E. Rasel, Self-alignment of a compact large-area atomic sagnac interferometer, *New J. Phys.* **14**, 015002 (2012).
- [23] A. V. Rakholia, H. J. McGuinness, and G. W. Biedermann, Dual-axis high-data-rate atom interferometer via cold ensemble exchange, *Phys. Rev. Applied* **2**, 054012 (2014).
- [24] J. Davis and F. Narducci, A proposal for a gradient magnetometer atom interferometer, *J. Mod. Opt.* **55**, 3173-3185 (2008).
- [25] M.-K. Zhou, Z.-K. Hu, X.-C. Duan, B.-L. Sun, J.-B. Zhao, and J. Luo, Precisely mapping the magnetic field gradient in vacuum with an atom interferometer, *Phys. Rev. A* **82**, 061602 (2010).
- [26] Z.-K. Hu, X.-C. Duan, M.-K. Zhou, B.-L. Sun, J.-B. Zhao, M.-M. Huang, and J. Luo, Simultaneous differential measurement of a magnetic-field gradient by atom interferometry using double fountains, *Phys. Rev. A* **84**, 013620 (2011).
- [27] B. Barrett, I. Chan, and A. Kumarakrishnan, Atom-interferometric techniques for measuring uniform magnetic field gradients and gravitational acceleration, *Phys. Rev. A* **84**, 063623 (2011).
- [28] J. B. Fixler, G. Foster, J. McGuirk, and M. Kasevich, Atom interferometer measurement of the newtonian con-

- stant of gravity, *Science* **315**, 74-77 (2007).
- [29] G. Lamporesi, A. Bertoldi, L. Cacciapuoti, M. Prevedelli, and G. Tino, Determination of the newtonian gravitational constant using atom interferometry, *Phys. Rev. Lett.* **100**, 050801 (2008).
  - [30] G. Rosi, F. Sorrentino, L. Cacciapuoti, M. Prevedelli, and G. Tino, Precision measurement of the newtonian gravitational constant using cold atoms, *Nature* **510**, 518-521 (2014).
  - [31] S. Fray, C. A. Diez, T. W. Hänsch, and M. Weitz, Atomic interferometer with amplitude gratings of light and its applications to atom based tests of the equivalence principle, *Phys. Rev. Lett.* **93**, 240404 (2004).
  - [32] A. Bonnin, N. Zahzam, Y. Bidel, and A. Bresson, Simultaneous dualspecies matter-wave accelerometer, *Phys. Rev. A* **88**, 043615 (2013).
  - [33] A. Bonnin, N. Zahzam, Y. Bidel, and A. Bresson, Characterization of a simultaneous dual-species atom interferometer for a quantum test of the weak equivalence principle, *Phys. Rev. A* **92**, 023626 (2015).
  - [34] D. Schlippert, J. Hartwig, H. Albers, L. L. Richardson, C. Schubert, A. Roura, W. P. Schleich, W. Ertmer, and E. M. Rasel, Quantum test of the universality of free fall, *Phys. Rev. Lett.* **112**, 203002 (2014).
  - [35] M. Tarallo, T. Mazzoni, N. Poli, D. Sutyryn, X. Zhang, and G. Tino, Test of einstein equivalence principle for 0-spin and half-integer-spin atoms: Search for spin-gravity coupling effects, *Phys. Rev. Lett.* **113**, 023005 (2014).
  - [36] L. Zhou, S. Long, B. Tang, X. Chen, F. Gao, W. Peng, W. Duan, J. Zhong, Z. Xiong, J. Wang et al., Test of equivalence principle at  $10^{-8}$  level by a dual-species double-diffraction raman atom interferometer, *Phys. Rev. Lett.* **115**, 013004 (2015).
  - [37] J. G. Williams, S. G. Turyshev, and D. H. Boggs, Progress in lunar laser ranging tests of relativistic gravity, *Phys. Rev. Lett.* **93**, 261101 (2004).
  - [38] S. Schlamminger, K.-Y. Choi, T. Wagner, J. Gundlach, and E. Adelberger, Test of the equivalence principle using a rotating torsion balance, *Phys. Rev. Lett.* **100**, 041101 (2008).
  - [39] R. Colella, A. W. Overhauser, and S. A. Werner, Observation of gravitationally induced quantum interference, *Phys. Rev. Lett.* **34**, 1472 (1975).
  - [40] C. Lämmerzahl, Quantum tests of the foundations of general relativity, *Class. Quantum. Grav.* **15**, 13 (1998).
  - [41] S. Dimopoulos, P. W. Graham, J. M. Hogan, and M. A. Kasevich, General relativistic effects in atom interferometry, *Phys. Rev. D* **78**, 042003 (2008).
  - [42] X.-C. Duan, X.-B. Deng, M.-K. Zhou, W.-J. Xu, F. Xiong, Y.-Y. Xu, C.-G. Shao, J. Luo, and Z.-K. Hu, Test of the universality of free fall with atoms in different spin orientations, *arXiv preprint arXiv:1602.06377* (2016).
  - [43] A. Sugarbaker, S. M. Dickerson, J. M. Hogan, D. M. Johnson, and M. A. Kasevich, Enhanced atom interferometer readout through the application of phase shear, *Phys. Rev. Lett.* **111**, 113002 (2013).
  - [44] C. Kuhn, G. McDonald, K. Hardman, S. Bennetts, P. Everitt, P. Altin, J. Debs, J. Close, and N. Robins, A bose-condensed, simultaneous dualspecies machZehnder atom interferometer, *New J. Phys.* **16**, 073035 (2014).
  - [45] D. Aguilera, H. Ahlers, B. Battelier, A. Bawamia, A. Bertoldi, R. Bondarescu, K. Bongs, P. Bouyer, C. Braxmaier, L. Cacciapuoti et al., STE-QUEST-test of the universality of free fall using cold atom interferometry, *Class. Quantum. Grav.* **31**, 115010 (2014).
  - [46] B. Altschul, Q. G. Bailey, L. Blanchet, K. Bongs, P. Bouyer, L. Cacciapuoti, S. Capozziello, N. Gaaloul, D. Giulini, J. Hartwig et al., Quantum tests of the einstein equivalence principle with the steQuest space mission, *Adv. Space Res.* **55**, 501-524 (2015).
  - [47] G. Foster, J. Fixler, J. McGuirk, and M. Kasevich, Method of phase extraction between coupled atom interferometers using ellipse-specific fitting, *Opt. Lett.* **27**, 951-953 (2002).
  - [48] J. K. Stockton, X. Wu, and M. A. Kasevich, Bayesian estimation of differential interferometer phase, *Phys. Rev. A* **76**, 033613 (2007).
  - [49] G. Varoquaux, R. A. Nyman, R. Geiger, P. Cheinet, A. Landragin, and P. Bouyer, How to estimate the differential acceleration in a two-species atom interferometer to test the equivalence principle, *New J. Phys.* **11**, 113010 (2009).
  - [50] X. Chen, J. Zhong, H. Song, L. Zhu, J. Wang, and M. Zhan, Proportional-scanning-phase method to suppress the vibrational noise in nonisotope dual-atom-interferometer-based weak-equivalence-principle tests experiments, *Phys. Rev. A* **90**, 023609 (2014).
  - [51] F. P. Dos Santos, Differential phase extraction in an atom gradiometer, *Phys. Rev. A* **91**, 063615 (2015).
  - [52] B. Barrett, L. Antoni-Micollier, L. Chichet, B. Battelier, P.-A. Gominet, A. Bertoldi, P. Bouyer, and A. Landragin, Correlative methods for dualspecies quantum tests of the weak equivalence principle, *New J. Phys.* **17**, 085010 (2009).
  - [53] A. Clairon, P. Laurent, G. Santarelli, S. Ghezali, S. Lea, and M. Bahoura, A cesium fountain frequency standard: preliminary results, *IEEE Trans. Instrum. Meas.* **44**, 128-131 (1995).
  - [54] P. Cheinet, F. P. Dos Santos, T. Petelski, J. Le Gouët, J. Kim, K. Therkildsen, A. Clairon, and A. Landragin, Compact laser system for atom interferometry, *Appl. Phys. B* **84**, 643-646 (2006).
  - [55] S. Merlet, J. Le Gouët, Q. Bodart, A. Clairon, A. Landragin, F. P. Dos Santos, and P. Rouchon, Operating an atom interferometer beyond its linear range, *Metrologia* **46**, 87 (2009).
  - [56] M.-K. Zhou, B. Pelle, A. Hilico, and F. P. dos Santos, Atomic multiwave interferometer in an optical lattice, *Phys. Rev. A* **88**, 013604 (2013).
  - [57] X. Li, C.-G. Shao, and Z.-K. Hu, Raman pulse duration effect in highprecision atom interferometry gravimeters, *J. Opt. Soc. Am. B* **32**, 248-257 (2015).
  - [58] P. Cheinet, B. Canuel, F. P. D. Santos, A. Gauguier, F. Yver-Leduc, and A. Landragin, Measurement of the sensitivity function in a timedomain atomic interferometer, *IEEE Trans. Instrum. Meas.* **57**, 1141-1148 (2008).